Lightweight high-brightness helmet-mounted head-up display system

Mathieu Wagner[a], Thibault North[a], Stéphane Bourquin[a], and Lucio Kilcher[b]

[a]Institut des Sciences et Technologies Industrielles, hepia, Member of the HES-SO University of Applied Sciences, Western Switzerland, 4, rue de la Prairie, CH–1202 Genève, Switzerland
[b]Lemoptix SA, Switzerland

ABSTRACT

We present a compact binocular head-up display for integration in a motorcycle helmet. A 2D MEMS-mirror reflecting laser beams enables the formation of a bright image superimposed on the user vision by means of retinal scanning. A 3d-printed prototype including the required optical components is presented and characterized. It fits the morphology of most users thanks to several degrees of freedom accessible to the user for fine-tuning.

Keywords: Heads-up displays, Lens system design, Optomechanics, First-order optics, 2D MEMS mirror

1. INTRODUCTION

Lately, Head-Mounted Displays (HMDs) have proven useful in many areas such as medicine and avionics.[1–5] The current trend towards wearable computing gives a new momentum to HMDs, as confirmed by the number of recent prototype of glasses by Google and others. Mostly, recent HMD designs have been industrialized in the form of glasses, superimposing information over the user's field of vision (FOV) via optical components such as beam-splitters, wedge prisms, or other kinds of free-form elements.[6–8] Challenges associated to the conception of such optical systems are numerous. HMDs must be lightweight, preserve the user FOV, fit to his morphology, a provide a virtual image with sufficient brightness in all light conditions. Another common problem is the size of the eyebox, defined as the area inside which the virtual image is perceived.[9] Some HMD systems are also designed for augmented reality, in which case they must display a wide-angle image approaching the eye FOV so that virtual objects or information can be mapped to objects of the real-world view.[10–12] More popular, other kinds of HMD systems are designed for hand-free interaction with electronic devices. A narrower FOV is sufficient for these systems, which are easily miniaturized and therefore less invasive.[13,14] Requirements associated to Helmet-Mounted Display Systems (HMDSs) belong to the this last class of devices. It is strictly necessary that the user FOV remains cleared of all bulky optical element: the FOV must be cleared on at least 210°×52° according to UN recommendation E/ECE/TRANS/505 No. 22, and for security purposes, no optical component should be close to the user eyes.

In this paper, we present a new binocular HMDS targeting motorcycle user. We describe its optical system and 3D-printed module, and show that it provides a high-brightness image even in daylight conditions. Moreover, the system is non-obtrusive and light. Only a few HMDS for motorcycle users where reported to date. The most promising system is perhaps the one of Livemap (livemap.info). According to the documents available on their website, their optical system is located on top of the helmet. It thereby expands its height and decreases in particular the vertical FOV. Nevertheless this design is said to satisfy the UN regulation mentioned above. Other companies sell monocular HMDS for motorcyclists which mainly consist of the formation of a virtual image in the edge of the user vision. It is the case of Skully (skully.com), as well as Nuviz (ridenuviz.com). It seems that these systems are comparable to a Google Glass adapted to a helmet. Unfortunately, those designs are not binocular and may reduce the user FOV. Most reports of HMDSs, despite not always targeting motorcycle users, require bulky optical components which can hardly be integrated inside a commercial motorcycle helmet

Further author information: (Send correspondence to Stéphane Bourquin)
Stéphane Bourquin: E-mail: stephane.bourquin@hesge.ch

Advances in Display Technologies VI, edited by Liang-Chy Chien, Sin-Doo Lee, Ming Hsien Wu, Proc. of SPIE Vol. 9770, 97700F · © 2016 SPIE
CCC code: 0277-786X/16/$18 · doi: 10.1117/12.2203444

without conflicting with its security padding elements.[15,16] Moreover, such systems are unable to provide an image with sufficient brightness, since they relay a screen image formed by light-emitting diodes (LEDs).

In this work, we satisfy the requirements mentioned above via a design including a MEMS-based laser micro-projector. The projector was provided by Lemoptix SA. It permits the projection of an ultra-bright image, when the laser scans the retina of the user through an optical system.[17,18] A benefit of this approach is that it is not subject to unwanted speckle, unlike systems transmitting a laser projected image onto a screen. Despite a relatively small eyebox size inherent to such retinal projection systems, the user eye remains easily inside the eyebox thanks to the tight adjustment of the helmet on the head and the inclusion of alignment knobs. The mechanical module containing the optical system is compact so that it can fit inside a commercial helmet without the removal of mandatory security padding elements. The location of the module at the bottom of the helmet also seem to be an original contribution to HMDS. The user FOV is therefore preserved.

Finally, we present here the simple optical design based on common optical components in a Keplerian telescope configuration.

2. OPTICAL SYSTEM

Fig. 1(a) and (b) depicts the optical system under paraxial approximation. Lenses are achromatic, and their configuration is similar to the one of a Keplerian telescope. However, the fact that the laser RGB micro-projector of Ref.[19] sends parallel laser rays from a point that is close to the first lens allows for the creation of an eyebox at a configurable position.The projected image has a ratio of 4:3 image and a half projection angle of $\alpha = 15°$. The projector MEMS faces a first converging lens l_1. This lens is followed by a second converging lens l_2. To form a virtual image at infinity, the output beam must also feature parallel rays. Therefore, the distance $\overline{l_1 l_2}$ is equal to the sum of the focal lengths $f_{1,2}$ of $l_{1,2}$. In this case, rays from different angles in the range $-\alpha \,..\, \alpha$ intersect at a distance g of l_2, where the user eye is placed. The system is binocular, and therefore this optical system is present twice in the optical module. The beam is split after the first lens, so that a correct inter-pupillary distance exists between the two beams. Fig. 1(b) shows the complete simulated optical system. A beam splitter and aluminum mirrors are used to redirect the images towards each eye, via two arms $A_{1,2}$.

The distance i_p between these two arms is set a standard inter-pupillary distance of 65 mm.[20] This distance is nevertheless adjustable to match most user's physiognomy. i_p can be varied by ± 10 mm. The distance $\overline{l_1 l_2}$ is tunable accordingly in order to preserve or adjust the focus. Finally, mirrors M_1 and M_2 can be rotated around axes y and $\vec{e_x} \pm \vec{e_z}$ to adjust the relative position of each virtual image, and an additional degree of freedom is provided to adjust the eyebox position in the z axis. The small-angle approximation is used since the half projection angle of $\alpha = 15°$, induces only an error of 2.2%. These first-order optics approximation allow the retrival of values for the lens diameters as well as their focal lengths. The virtual image is seen under an angle $\beta = \alpha f_1/f_2$, and hence only depends on the projection angle and the focal ratios. The half-width i_1 on lens l_1 only depends on α and f_1. Similarly, the half-width i_2 on lens l_2 depends on the focal lengths $f_{1,2}$, as well as the distance d between the projector and lens l_1, as written in Eqs. (1) and (2):

$$i_1 = \tan(\alpha) d \approx \alpha d \tag{1}$$

$$\begin{aligned} i_2 &= i_1 + \tan(\gamma)(f_1 + f_2) \approx \alpha d + \gamma(f_1 + f_2) \\ &= \alpha \left(f_1 + f_2 - d\frac{f_2}{f_1} \right) \end{aligned} \tag{2}$$

with:

$$\gamma = \arctan\left(\frac{e}{f_1}\right) \approx \frac{e}{f_1} = \alpha \frac{f_1 - d}{f_1} \tag{3}$$

The point where parallel rays meet, at a distance g of the last lens l_2 depends on the focal lengths $f_{1,2}$ and the projector distance d to the lens l_1. Shifting the projector along $\vec{e_z}$ enables an adjustment of the eyebox position

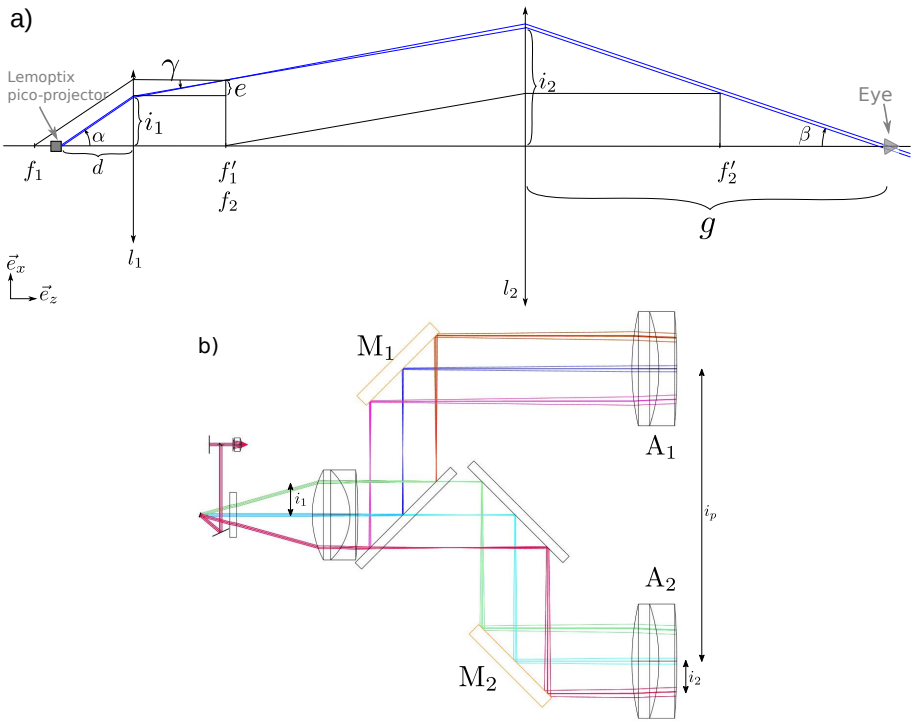

Figure 1. Optical schematic of the system. (a) ray tracing in paraxial approximation, (b) final optical layout.

in the z direction, independently of β. Likewise, given two focal lengths and lens sizes, the distance d can be determined from the effective image half-width on lens l_2:

$$g \approx f_2 + \frac{f_2^2}{f_1} - d\frac{f_2^2}{f_1^2} \tag{4}$$

$$d \approx \frac{f_1}{f_2}\left(f_1 + f_2 - \frac{i_2}{\alpha}\right) \quad \text{with } i_2 > i_1 \tag{5}$$

A rectangular image of 7°×5° is formed onto the user field of vision, at its bottom. A relatively small image size and an adequate position ensure that the user is not disturbed by the virtual image. The projector is placed such that $d = f_1$, and output beams converge at f_2. In this system, the focal lengths are $f_1 = 20$ mm, and $f_2 = 90$ mm. The width of l_2 as well as the eyebox position are computed via (2)–(5), and hence $i_1 = 5.2$ mm, and $i_2 \in 4.05 \,..\, 6.41$ mm, $g \in 70 \,..\, 110$ mm when $d \in 21 \,..\, 19$ mm. Fig. 2 depicts the 3D-printed mechanical system that was designed to host the optical components.

3. 3D-PRINTED OPTO-MECHANICAL SYSTEM

Fig. 2(b) indicates that slight color difference occur in each arm mainly because of a non-flat response of the beam-splitter. Nevertheless, the color intensity difference between each image does not exceeds 3%. Visually, this difference can not be noticed. The optical system described above imposes tight constraints on the mechanical system. Fortunately, the flexibility provided by the 3D-printing process enables the integration of all optical components without collision in the reduced volume of the module. Details of the printed system are depicted in Fig. 3.

On the helmet visor, the image is relayed by two plastic plates. A surface of ≈ 2.5 cm^2 is required per eye on these plastic plates, without the need for any reflection coating. Fresnel reflection on these plates is sufficient since the amount of optical power from the projector is large. The plastic plates are in a common plane, for simplicity and ease of integration. Fig. 4 shows the module integrated in the helmet, requiring an optical path length of $g \approx 90$ mm towards the user eye.

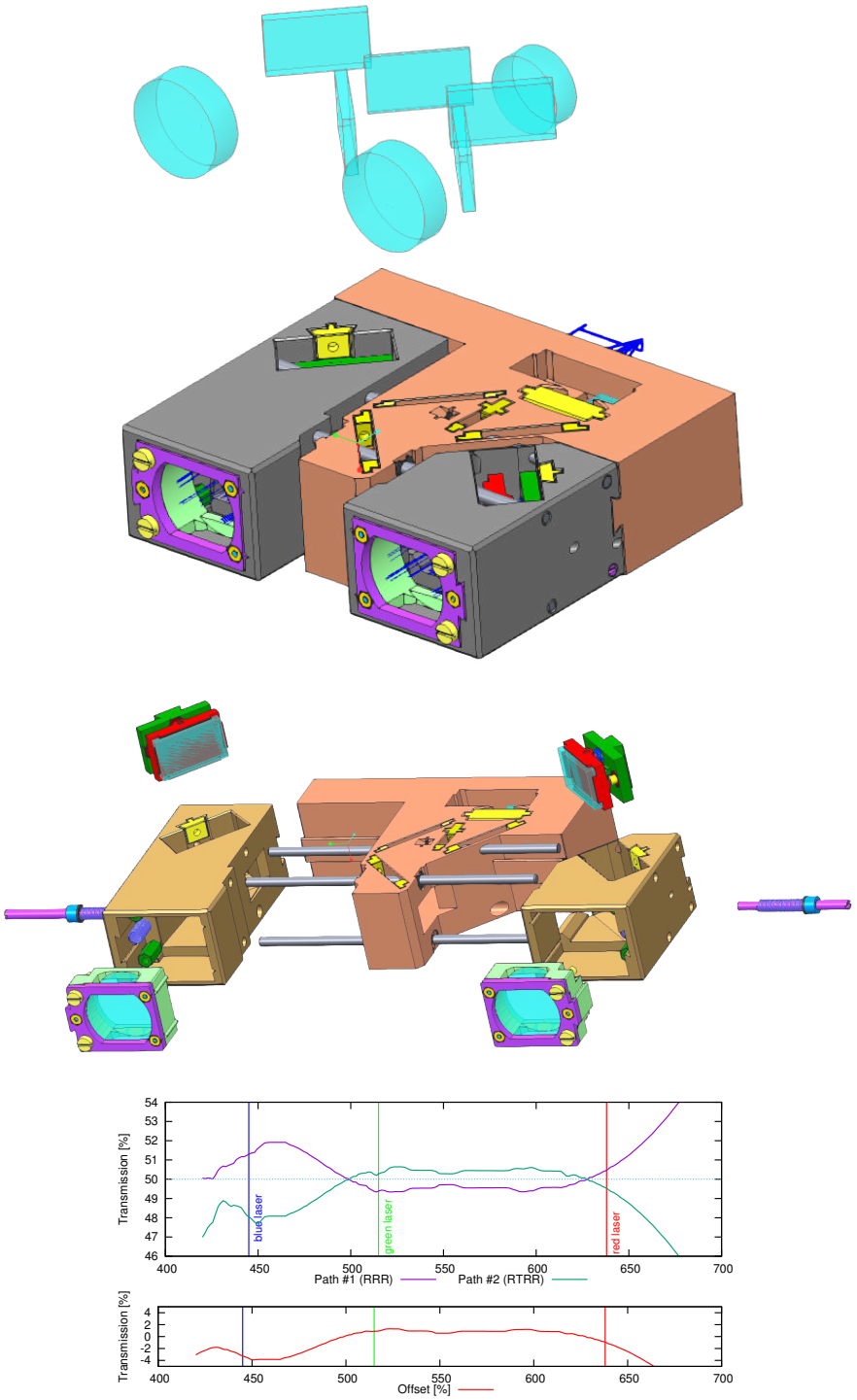

Figure 2. (a) Prototype and its optics, and its explded view. 8 degrees of freedom include one translation as well as two rotations per arm. (b) per arm light transmission as a function of wavelength. R: reflection, T: transmission.

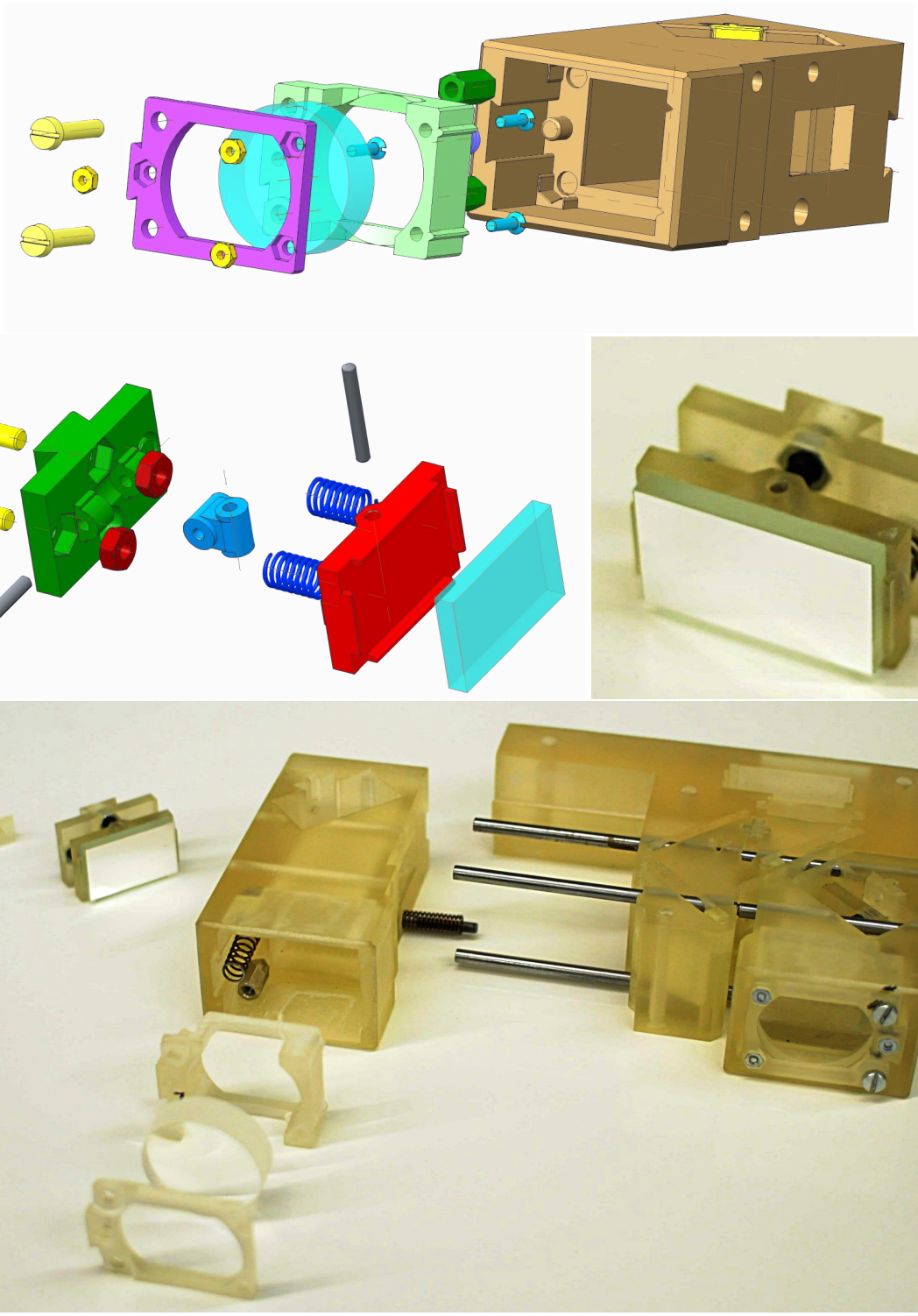

Figure 3. Subsystems details: (top) front lens of the right arm, (middle) mirror mount, (bottom) Exploded view of the prototype.

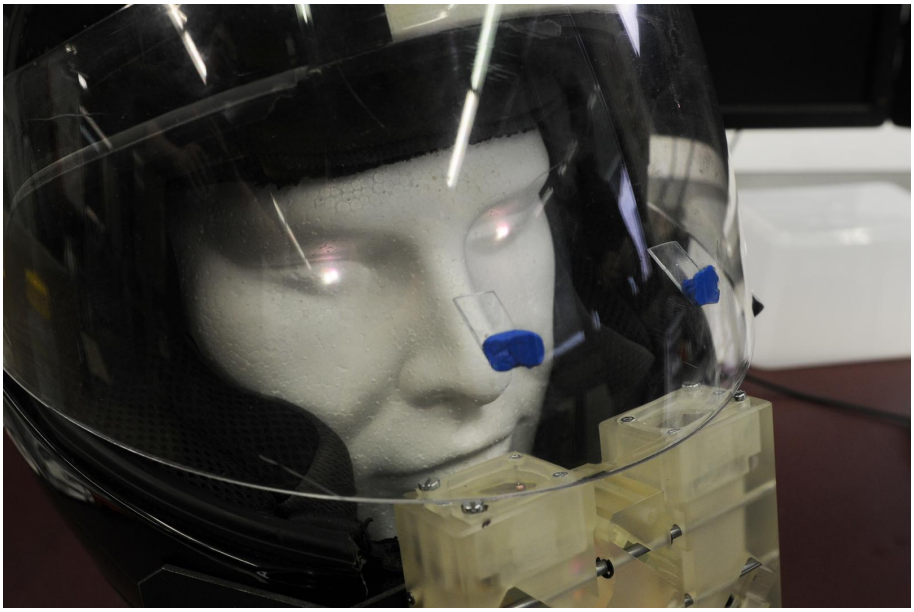

Figure 4. HMD system mounted in a standard helmet. The filters are removed to illustrate the beam path toward the user eye and the required size of the plastic plates. Only the external plastic chin piece was removed, and all shock-absorbing parts are conserved.

4. RESULTS

A camera was placed inside the helmet to produce Fig. 5(a). The virtual image as seen outside on a sunny day. In this configuration, a 30 dB neutral density (ND) filter is set after the projector. In Fig. 5(b), the virtual image is seen indoors, with a higher attenuation of 34.7 dB.

To verify that the image is not altered throughout the optical system, the image of the projector S, projected onto a wall, is compared with the image I_o as seen from inside the helmet. In Fig. 5(c), key-points are selected in image S (green), and corresponding key-points are found on I_o, (black crosses). One can see minor image deformations can be seen. These deformations are mainly due to the fact that the light beam reaching lenses $A_{1,2}$ does not always coincides with their optical axes, since they depend on the adjustment of mirrors $M_{1,2}$. Fig. 5(d) shows the spot diagram of the simulated optical system. The spot is evaluated on the retina, for each of the three wavelengths of the system. Since the wavelength difference between the blue and the red is of 193 nm, it is expected that different wavelengths focus at different z-values.

5. CONCLUSION

We have reported a new HMDS targeting motorcycle users. The system is binocular and has a good compactness of $\sim 1/3$ of a liter. It fits inside a standard helmet, and provides sufficient luminosity for daylight conditions. Several degrees of freedom are provided to adjust the system for different users. A virtual image of a size of $7^\circ \times 5^\circ$, is visible in the bottom of the user FOV.

Acknowledgment

The authors would like to thanks Lemoptix SA for lending the laser projector as well as Dominique Marchal of Lemoptix for insightful discussions. This work was supported by the Swiss Innovation Promotion Agency CTI, as project 13916 entitled "High brightness, ultra-miniature Head-Mounted Display systems".

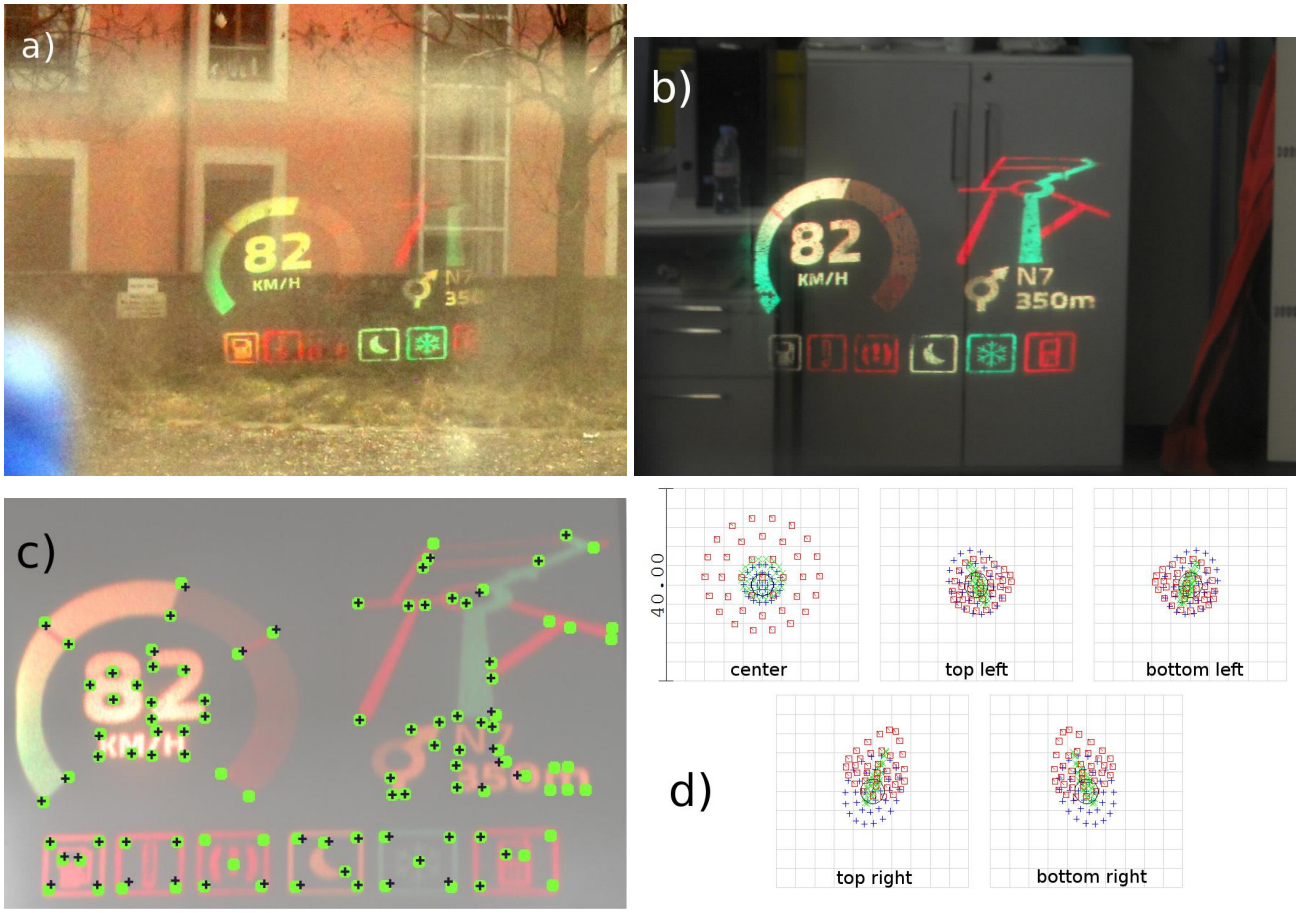

Figure 5. (a) Picture taken outside, on a sunny day. The filters provide an attenuation of 30 dB. Vignetting comes from the camera; the image is fully visible with human eyes. (b) Picture taken from the helmet, indoors, with an attenuation of 34.7 dB. (c) Image projected onto a wall (green keypoints) compared with the image seen from the helmet (black crosses), corresponding to picture (a). (d) Spot diagram simulated on the retina (scale in µm). Colors corresponds to the three wavelengths: blue 445 nm, green 515 nm, red 638 nm.

REFERENCES

[1] Fuchs, H., Livingston, M., Raskar, R., Colucci, D., Keller, K., State, A., Crawford, J., Rademacher, P., Drake, S., and Meyer, A., [Augmented reality visualization for laparoscopic surgery], vol. 1496 of Lecture Notes in Computer Science, Springer Berlin Heidelberg (1998).

[2] Rolland, J. P. and Fuchs, H., "Optical versus video see-through head-mounted displays in medical visualization," Presence: Teleoperators and Virtual Environments **9**(3), 287–309 (2000).

[3] Azuma, R., Baillot, Y., Behringer, R., Feiner, S., Julier, S., and MacIntyre, B., "Recent advances in augmented reality," Computer Graphics and Applications, IEEE **21**(6), 34–47 (2001).

[4] Rolland, J. P., Biocca, F., Hamza-Lup, F., Ha, Y., and Martins, R., "Development of head-mounted projection displays for distributed, collaborative, augmented reality applications," Presence: Teleoperators and Virtual Environments **14**(5), 528–549 (2005).

[5] Keller, K., State, A., and Fuchs, H., "Head mounted displays for medical use," J. Display Technol. **4**, 468–472 (Dec 2008).

[6] Cheng, D., Wang, Y., Hua, H., and Talha, M. M., "Design of an optical see-through head-mounted display with a low f-number and large field of view using a freeform prism," Appl. Opt. **48**, 2655–2668 (May 2009).

[7] Liu, S., Hua, H., and Cheng, D., "A novel prototype for an optical see-through head-mounted display with addressable focus cues," IEEE Transactions on Visualization and Computer Graphics **16**(3), 381–393 (2010).

[8] Van Krevelen, D. and Poelman, R., "A survey of augmented reality technologies, applications and limitations," International Journal of Virtual Reality **9**(2), 1 (2010).

[9] Boger, Y., "The 2008 hmd survey: Are we there yet," White paper published by Sensics Inc. URL: http://www.sensics.com/files/documents/2008SurveyResults.pdf (2008).

[10] Cheng, D., Wang, Y., Hua, H., and Sasian, J., "Design of a wide-angle, lightweight head-mounted display using free-form optics tiling," Opt. Lett. **36**, 2098–2100 (Jun 2011).

[11] Hua, H., Hu, X., and Gao, C., "A high-resolution optical see-through head-mounted display with eyetracking capability," Opt. Express **21**, 30993–30998 (Dec 2013).

[12] Yang, J., Liu, W., Lv, W., Zhang, D., He, F., Wei, Z., and Kang, Y., "Method of achieving a wide field-of-view head-mounted display with small distortion," Opt. Lett. **38**, 2035–2037 (Jun 2013).

[13] Kerr, S. J., Rice, M. D., Teo, Y., Wan, M., Cheong, Y. L., Ng, J., Ng-Thamrin, L., Thura-Myo, T., and Wren, D., "Wearable mobile augmented reality: Evaluating outdoor user experience," in [Proceedings of the 10th International Conference on Virtual Reality Continuum and Its Applications in Industry], VRCAI '11, 209–216, ACM, New York, NY, USA (2011).

[14] Koss, B. and Sieber, A., "Head-mounted display for diving computer platform," Display Technology, Journal of **7**, 193–199 (April 2011).

[15] Rolland, J. and Hua, H., "Head-mounted display systems," Encyclopedia of optical engineering , 1–13 (2005).

[16] Cakmakci, O. and Rolland, J., "Head-worn displays: a review," Display Technology, Journal of **2**, 199–216 (Sept 2006).

[17] Tidwell, M., Johnston, R. S., Melville, D., and Furness, T., "The virtual retinal display-a retinal scanning imaging system," Proceedings of virtual reality World **95**, 325–333 (1995).

[18] Pryor, H. L., Furness, T. A., and Viirre, E., "The virtual retinal display: A new display technology using scanned laser light," Proceedings of the Human Factors and Ergonomics Society Annual Meeting **42**(22), 1570–1574 (1998).

[19] Kilcher, L. and Abelé, N., "MEMS-based microprojection system with a 1.5cc optical engine," in [SPIE MOEMS-MEMS], Proc. SPIE **8252**, 825204–825204, International Society for Optics and Photonics (2012).

[20] Dodgson, N. A., "Variation and extrema of human interpupillary distance," in [Electronic Imaging 2004], Proc. SPIE **5291**, 36–46, International Society for Optics and Photonics (2004).